euronoise

Axisymmetrical and non axisymmetrical guided waves propagating in a solid elastic cylinder embedded in a solid medium

Slah Yaacoubi[a], Laurent Laguerre[a], Eric Ducasse[b] and Marc Deschamps[b]

[a]LCPC, Lab. Central des Ponts et chaussées (LCPC), Route de Bouaye-BP 4129, 44341 Bouguenais, France

[b]LMP, Lab. de Mécanique et Physique (LMP), 351, Place de la Libération, 33405 Talence, France

slah.yaacoubi@lcpc.fr

The aim of this paper is to derive the space-time velocity field in a cylindrical waveguide perfectly embedded in an infinite medium and generated by an inside bounded beam. This beam is generated by an off-axis source. It is up to us to generate non-axisymmetric waves. Vector Hankel transform and Fourier series are combined to decompose the inside field into infinity of elementary cylindrical waves propagating in radial direction and planar waves propagating in axial direction. Global resolution method and Generalized Debye series expansion are both used to calculate the global cylindrical reflection and transmission coefficients. Numerical results of the non-axisymmetric propagated waves are discussed.

1 Introduction

Many structures in civil engineering notably bridges and nuclear power plants (NPP) must be regularly, strictly and carefully controlled. The nature of such structures necessitates a non-destructive testing procedure. This has led many researchers to study ultrasonic guided waves techniques among others for the purpose of non-destructive inspection of structures. This technique is appealing because it can provide a rapid, accurate and inexpensive assessment in a wide range of industries. But, there are some difficulties in applying this technique. One prominent difficulty is the presence of elastic or viscoelastic embedding medium. These embeddings tend to attenuate the propagating energy. This can severely degrade the performance of guided wave test with regard to test sensitivity and the distance of propagation.

Generated guided waves can be controlled by source loadings. Indeed, when a source loading is axisymmetric and localized on the axis of revolution, only axisymmetric waves are generated. But when a source loading is non-axisymmetric or axisymmetric localised in an off-axis position, the generated fields include all the propagation waves. For both cases, the field amplitude depends on source loading conditions.

Due to the complicated nature non-axisymmetric guided waves, non axisymmetric sources loading is avoided in non-destructive evaluation (NDE) applications. However, there are some cases where only a part of bar is accessible and thus only an-off axis source can be applied. Additionally, when axisymmetric guided waves are generated, the reflected waves from defects will be non-axisymmetric due to the irregular geometries of defects. For that reason, investigation of non-axisymmetric guided waves becomes an interesting subject for both source loading study and defect characterization.

Danthez et al. [1] have studied the propagation of axisymmetric waves in a free cylindrical waveguide with the aim of the NDE. This study has been extended by Laguerre et al. [2] to include the propagation in a cylinder embedded in an unbounded medium. They have shown the existence of attenuation due to leakage in that medium.

In this paper, we study the propagation of non-axisymmetric and axisymmetric guided waves in cylindrical waveguide embedded in an unbounded medium. A source can be moved for generating such a wave type. A theoretical development based on Vector Hankel Transform, Fourier series and Generalized Debye series is carried out in Sec.3. This development is highlighted by one numerical example in Sec.4. Numerical results and discussions are presented in Sec.5. Finally, the conclusions are mentioned in Sec. 6.

2 Problem statement

Let us consider an elastic, homogeneous and isotropic cylinder of infinite length, radius b, and density ρ. As shown in Fig.1. A cylindrical coordinate system (r,θ,z) is chosen with the z-direction coincident with the axis of the cylinder. This cylinder is embedded in an infinite elastic medium which is homogeneous and isotropic.

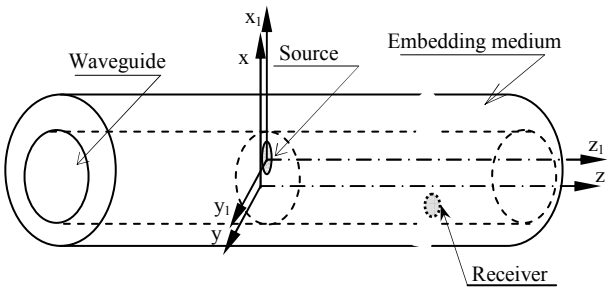

Fig1 : Problem geometry

The source of characteristic radius *a* is localized in an off-axis revolution of a cylinder. It is assumed that the source distribution is of the circular axial symmetry in its own basis $\left(o_1,\vec{e}_{r_1},\vec{e}_{\theta_1}\right)$.

3 Resolution steps

For detecting defects in a cylinder, it is useful to understand the acoustic field generated by the source. One traditional method for solving this problem employs a classical normal mode expansion method [3-5]. But this method is not suitable when there is transmission (leakage) into surrounding medium with the shear velocity smaller than that of the waveguide. In such a case, the orthogonality relations underlying the normal mode expansion method are not directly applicable. Instead of using this method, we use here the integral transform method.

3.1 Vector Hankel Transform for decomposing an incident field

In the general case, the sound beam is non uniform in the (r,θ) plane which is parallel to the propagation direction. The sound field of such an incident beam can be expressed as the sum of infinite cylindrical waves by using the combination of Fourier series and Vector Hankel Transform

[6-7]. The incident particle velocity vector $\vec{v}^{inc}$ can be given thus by:

$$\vec{v}^{inc}(r,\theta,z) = \sum_{n=-\infty}^{+\infty} \vec{v}_n(r,z) e^{in\theta} \quad (1)$$

where

$$\vec{v}_n(r,z) = \int_0^{\infty} \Im(k_r r) \vec{V}_n(k_r,z) k_r dk_r \quad (2)$$

$\Im(k_r r)$ is a 3×3 matrix which is expressed as follows:

$$\Im(k_r r) = \begin{pmatrix} \mathrm{B}_2(k_r r) & \mathrm{B}_3(k_r r) & 0 \\ \mathrm{B}_3(k_r r) & \mathrm{B}_2(k_r r) & 0 \\ 0 & 0 & \mathrm{B}_1(k_r r) \end{pmatrix} \quad (3)$$

where

$$\begin{cases} \mathrm{B}_1(k_r r) = J_n(k_r r) \\ \mathrm{B}_2(k_r r) = \frac{1}{2}\left[J_{n-1}(k_r r) + J_{n+1}(k_r r)\right] \\ \mathrm{B}_3(k_r r) = \frac{1}{2}\left[-J_{n-1}(k_r r) + J_{n+1}(k_r r)\right] \end{cases} \quad (4)$$

J_n is a Bessel function of order n. n is the circumferential number. The radial wavenumber k_r is related to the radial space frequency by $k_r = 2\pi p$.

The vector Hankel transform of the incident particle vector velocity $\vec{V}_n(k_r,z)$ is the amplitude of each of the constituent cylindrical waves. When these cylindrical waves are summed, they are mathematically equivalent to the incident bounded beam amplitude distribution.

For the purpose of studying the influence of the polarization, each cylindrical wave can be decomposed into three partial waves: one longitudinal (L^n) and two shears (T_1^n and T_2^n). So $\vec{V}_n(k_r,z)$ can be expressed as a function of cylindrical waves amplitudes which are A_L^n, $A_{T_1}^n$ and $A_{T_2}^n$ respectively.

$$\begin{aligned} V_r^n(k_r,z) &= -k_r A_L^n(k_r) e^{-i2\pi w_L z} + i2\pi w_T A_{T_1}^n(k_r) e^{-i2\pi w_T z} \\ V_\theta^n(k_r,z) &= i2\pi w_T A_{T_1}^n(k_r) e^{-i2\pi w_T z} + k_r A_{T_2}^n(k_r) e^{-i2\pi w_T z} \\ V_z^n(k_r,z) &= -i2\pi w_L A_L^n(k_r) e^{-i2\pi w_L z} + k_r A_{T_1}^n(k_r) e^{-i2\pi w_T z} \end{aligned} \quad (5)$$

where w_L is the axial space frequency of L^n and w_T is that of T_1^n and T_2^n.

Since the knowledge of the beam field distribution in any plane specifies completely the value of the function $\vec{V}_n(p,z)$. The most convenient plane to use is the $z=0$ plane because the progressive term disappears (eq (5)). Hence, by using the inverse vector Hankel transform, $\vec{V}_n(p)$ can be determined:

$$\vec{V}_n(k_r) = 2\pi \int_0^{\infty} \Im(k_r r) \vec{v}_n(r,0) r dr \quad (6)$$

Finally, injecting this equation in equation system (5), the amplitudes A_L^n, $A_{T_1}^n$ and $A_{T_2}^n$ can be easily calculated.

The infinity of waves constructing the incident field will propagate through the waveguide. These individual waves undergo multiple interactions with waveguide/embedding interface. Consequently, the resulting field in such point M in the waveguide can be deduced from the incident vector velocity field by:

$$\vec{v}(\vec{r}) = \sum_{n=-\infty}^{+\infty} \int_0^{\infty} \vec{F}(k_r) \Im(k_r r) \vec{V}_n(k_r,z) k_r dk_r e^{in\theta} \quad (7)$$

$\vec{F}(k_r)$ is the (3×1) transfer function vector of the waveguide or more precisely of the part from the source to the receiver point M (Fig.1). $\vec{r} = (r,\theta,z)$ is the displacement vector. We note that the time part is omitted in this equation.

The total field can be expressed by:

$$\vec{v} = v_r \vec{e}_r + v_\theta \vec{e}_\theta + v_z \vec{e}_z \quad (8)$$

Its norm can be written as:

$$\|\vec{v}\| = \sqrt{v_r^2 + v_\theta^2 + v_z^2} \quad (9)$$

3.2 Global method resolution and Debye series

The global method calculations give a global description of the scattering. The multiple reflections at the surface waveguide and transmissions through the interface waveguide/embedding medium are not clear in the global formalism. The connection between the global theory and the ray acoustics is known as the Debye-series expansion. The Debye-series expansion allows for the decomposition of the global physical process in a series of local interactions, which can bring a better physical understanding than the global resolution.

The incident wave can be longitudinal (L^n), vertical shear (T_1^n) or horizontal shear (T_2^n). Each engenders three waves by reflection and three waves by transmission through waveguide/embedding medium interface.

Continuity conditions at this interface lead to a linear system of equations:

$$\underline{\underline{C}}^n \underline{X}_i^n = \underline{P}_i^n \quad , \left(i = L^n, T_1^n, T_2^n\right) \quad (10)$$

where

$$\underline{X}_i^n = \left\{X_{iL}^{n-}, X_{iT_1}^{n-}, X_{iT_2}^{n-}, X_{iL}^{n+}, X_{iT_1}^{n+}, X_{iT_2}^{n+}\right\}^{tr} \quad (11)$$

The superscript *tr* is for vector transposition.

The first three coefficients represent the global *reflection* coefficient vector $\underline{XR}_i^n$. The last three components represent the global *transmission* coefficient vector $\underline{XT}_i^n$.

$\underline{\underline{C}}^n$ represents the continuity matrix for each cylindrical wave. Its components are expressed in appendix I. $\underline{P}_i^n$ is the velocity-stress vector of the source.

By extending the Generalized Debye Series used in 2D study [2] for 3D study, the final explicit expression of $\underline{XR}_i^n$ (indicated by sign - above) is:

$$\begin{Bmatrix} X_{iL}^n \\ X_{iT_1}^n \\ X_{iT_2}^n \end{Bmatrix} = \sum_{N=1}^{\infty} \begin{bmatrix} r_{LL}^n & r_{T_1L}^n & r_{T_2L}^n \\ r_{LT_1}^n & r_{T_1T_1}^n & r_{T_2T^1}^n \\ r_{LT_2}^n & r_{T_1T^2}^n & r_{T_2T^2}^n \end{bmatrix}^{N-1} \begin{Bmatrix} r_{iL}^n \\ r_{iT_1}^n \\ r_{iT_2}^n \end{Bmatrix}, \qquad (12)$$

r_{ij}^n are the local reflection coefficients of a cylindrical wave by the waveguide/embedding interface, when *i* and *j* are the incident and reflected wave type respectively. *N* is the interactions number.

Eq.(12) retains explicitly the multiple interactions with the interface.

4 Numerical example

For studying the non-axisymmetric waves, the source is localized in an off-axis of the bar. A question can be asked: can we generate these waves by only an axial excitation?

So, the velocity field is expressed in the source basis by:

$$\vec{v}(r_1,t) = \left\{0, \quad 0, \quad v_z(r_1)\right\}^{tr} e(t) \qquad (13)$$

where, at $z=0$, v_z is a bounded Gaussian beam which is expressed as follows:

$$v_z = \begin{cases} v_0 \exp\left(-\dfrac{\pi r_1^2}{\alpha^2}\right), r_1 < a \; and \; \theta_1 \in [0,2\pi] \\ 0 \qquad , \qquad otherwise \end{cases} \qquad (14)$$

By using the addition theorem [8] and the inverse vector Hankel transform, the axial velocity component can be written in the global basis after simplification as follows:

$$v_z(r,\theta) = \sum_{n=-\infty}^{n=+\infty} \int_0^{+\infty} 2\pi p \alpha^2 v_0 e^{-\pi\alpha^2 p^2} B_1(2\pi pr) \times J_n(2\pi pr_0) e^{in(\theta-\theta_0)} dp, \; r \in [0,b] \; and \; \theta \in [0,2\pi] \qquad (15)$$

The propagation of the waves in the waveguide will create radial, tangential and axial motions. The velocity field in space-time domain can be expressed by:

$$v_z^{ij}(\vec{r},t) = \sum_{n=0}^{+\infty} \varepsilon \int_{-\infty}^{+\infty} \left\{ \int_0^{+\infty} 2\pi p \left[\eta + X_{ij}^n\right] \alpha^2 v_0 e^{-\pi\alpha^2 p^2} B_1(2\pi Qr) \times J_n(2\pi Qr_0) \cos n(\theta-\theta_0) e^{-I2\pi w_i z} \, dp \right\} E(f) e^{-I2\pi ft} df \qquad (16)$$

where: I is the imaginary number ($I^2 = -1$),

$$\varepsilon = \begin{cases} 1 \; if \;\; n = 0 \\ 2 \; if \;\; n > 0 \end{cases}, \qquad \eta = \begin{cases} 1 \; if \;\; i = j \\ 0 \; if \;\; i \neq j \end{cases},$$

$$Q = \begin{cases} p \;\; if \;\; i = j \;\; or \;\; ij = T_1^n T_2^n; T_2^n T_1^n \\ q_T(w_L) \; if \;\; i \neq j \;\; and \;\; i = L^n \\ q_L(w_T) \; if \;\; i \neq j \;\; and \;\; i = T_1^n, T_2^n \end{cases}$$

and

$$E(f) = \int_{-\infty}^{\infty} e(t) e^{i2\pi ft} dt \qquad (17)$$

where $e(t)$ is a modulated Gaussian input pulse of a constant carrier frequency f_c and pulse width $2T_s$, centred around time $t_0 > 0$. Its mathematical expression is given by:

$$e(t) = e^{-\left(\frac{(t-t_0)}{T_s}\right)^2} \sin(2\pi f_c t) \qquad (18)$$

The radius of the Gaussian pulse is chosen to be small $(\alpha = 2mm)$ for maximizing lateral surface interactions in order to reveal the waveguide propagation effect [2].
The material parameters are given in the table below.

Material	$c_L\,(ms^{-1})$	$c_T\,(ms^{-1})$	$\rho\,(kgm^{-3})$	radius (m)
Steel	5960	3260	7932	8.10^{-3}
Cement grout	2810	1700	1600	∞

Table 1: Material parameters

5 Results and discussions

Applying the Fast Fourier Transform (FFT) in Eq. (16) and equations given in abstract B with respect to z coordinate, the velocity can be expressed in (r,θ,w_z,f) domain, where w_z is the space axial frequency.

$$V(r,\theta,w_z,f) = \int_{-\infty}^{\infty} v(r,\theta,z,f) e^{i2\pi w_z z} dz \qquad (19)$$

The dispersion diagram is a representation of the velocity amplitude $|V|$ as a function of frequencies (w_z,f). For the sake of clarity, we represent the image of $|V|$ in the (w_z,f) plane. The result of this representation is illustrated by 2.a, 2.b, 2.c and 2.d figures. The first three simulated dispersion diagrams are superposed with dispersion curves (few lines). These curves are derived from Disperse software which is based on modal solutions. We observe a very good agreement between our dispersion diagrams and dispersion curves L(0,m), T(0,m) and F(1,m).

Since the excitation is only longitudinal, the simulated signal phase velocities describe only the portion of the

dispersion curves greater than the velocity of longitudinal wave in steel c_L.

In spite of the axial excitation (only the v_z component is not zero), all types of modes are excited: longitudinal L(0,m), torsional T(0,m) and flexural F(n,m), *n*>0. The generation of flexural modes is due to off-axis source positioning. In addition, in some cases, the non-axisymmetric wave amplitude $(n > 0)$ is greater than that of axisymmetric wave. This is shown in Fig.3 which plots the maximum of the velocity amplitude as a function of the circumferential number *n* for r_0=5mm and r=8mm.

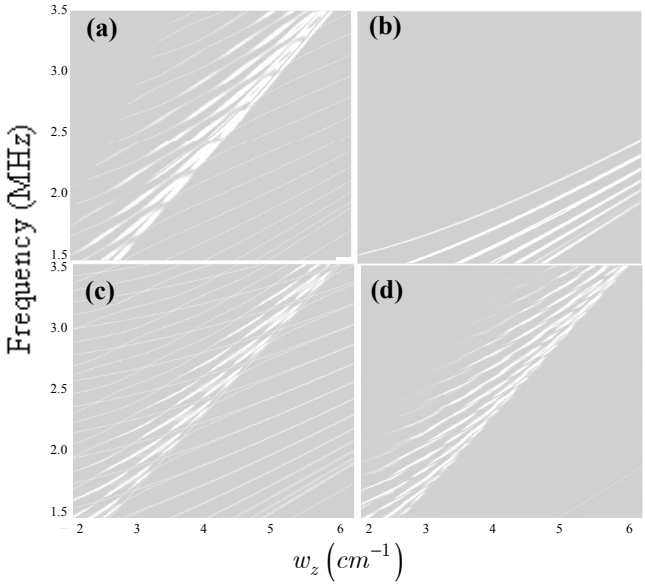

Fig.2: Velocity dispersions diagrams (w_z, f) and dispersion curves simulated by Disperse software for $z_0 = 110mm$ and f_0=2.5MHz : (a) longitudinal modes L(0,m), (b) Torsional modes T(0,m), (c) flexural modes F(1,m) and (d) total velocity (sum of all modes).

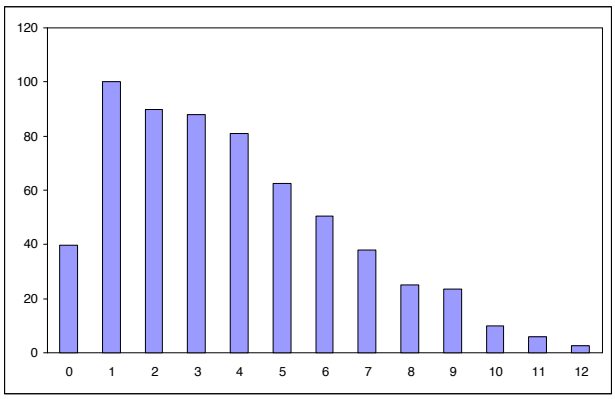

Fig.3: Maximum of the amplitude velocity as a function of circumferential number *n* for $r_0 = 5mm$. It's defined as a percentage of the greatest amplitude velocity (n=1).

Figure 4 plots a normalized time waveform of velocity for the steel waveguide embedded in cement grout for the circumferential number n=1. A source is localized at many position $r_0 = 0$ while θ_0 is fixed at zero for all cases. We observe that the time waveform amplitudes decrease when the coordinate r_0 decrease. This is due to the reduced path between source and receiver point.

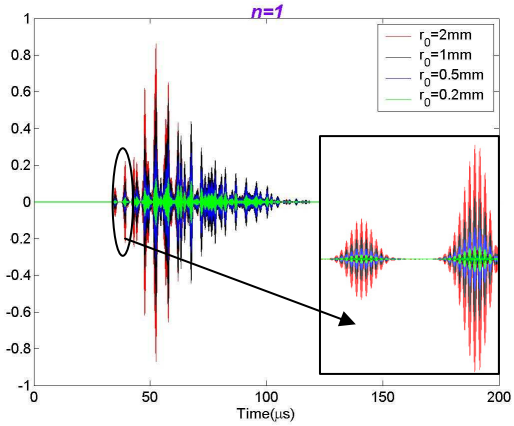

Fig.4: Time waveforms of velocity for the steel waveguide embedded in cement grout for n=1 and some r_0 (0.2, 0.5, 1, 2mm). The point receiver is at r=8mm, z=200mm and $\theta = 0$.

6 Conclusion

A theoretical development of a three-dimensional bounded beam travelling in a cylindrical solid waveguide embedded in an infinite medium has been presented. This development is based on a combination of Vector Hankel Transform, Fourier Series and Generalized Debye Series (GDS). If the source is localized in an axis cylinder, only axisymmetric waves can be generated. Otherwise, non-axisymmetric waves are generated. For some source positionning, their amplitudes are greater than that of the axisymmetric waves. Therefore, non-axisymmetric waves deserve special attention when dealing with both source loading and defect detection and characterization.

Acknowledgments

The authors wish to thank l'Agence Nationale de la Recherche and Electricité de France Recherche et Développement for supporting this work.

Appendix A: The matrix elements of system (10)

$$a_{11} = -p_2 H_{n+1}^{(m)}(\alpha) + \frac{n}{2\pi b} H_n^{(m)}(\alpha)$$

$$a_{21} = -\frac{n}{2\pi b} H_n^{(m)}$$

$$a_{31} = -iw H_n^{(m)}$$

$$a_{41} = \frac{i2\pi}{\omega}\mu\left(\left(q_m^2 - w^2 + \frac{n(1-n)}{2\pi^2 b^2}\right)H_n^{(m)} - \frac{p_m}{\pi b} H_{n+1}^{(m)}\right)$$

$$a_{51} = \frac{n\mu}{i\omega}\left(\frac{1-n}{\pi b^2} H_n^{(m)}(\alpha) + \frac{2p_m}{b} H_{n+1}^{(m)}(\alpha)\right)$$

$$a_{61} = \frac{2\mu w}{\omega}\left(2\pi p_m H_{n+1}^{(m)}(\alpha) - \frac{n}{b} H_n^{(m)}(\alpha)\right)$$

$$a_{12} = iwH_{n+1}^{(m)}(\beta)$$

$$a_{22} = iwH_{n+1}^{(m)}(\beta)$$

$$a_{32} = q_m H_n^{(m)}(\beta)$$

$$a_{42} = \frac{2\pi}{\omega}\mu w\left(2q_m H_n^{(m)}(\beta) - \frac{n+1}{\pi b}H_{n+1}^{(m)}(\beta)\right)$$

$$a_{52} = \frac{2\mu w}{\omega}\left(\pi q_m H_n^{(m)}(\beta) - \frac{n+1}{b}H_{n+1}^{(m)}(\beta)\right)$$

$$a_{62} = \frac{2\pi\mu}{i\omega}\left(\frac{nq_m}{2\pi b}H_n^{(m)}(\beta) - \left(q_m^2 - w^2\right)H_{n+1}^{(m)}(\beta)\right)$$

$$a_{13} = \frac{n}{2\pi b}H_n^{(m)}(\beta)$$

$$a_{23} = q_m H_{n+1}^{(m)} - \frac{n}{2\pi b}H_n^{(m)}$$

$$a_{33} = 0$$

$$a_{43} = \frac{2\pi n}{i\omega}\mu\left(\frac{n-1}{2\pi^2 b^2}H_n^{(m)}(\beta) - \frac{q_m}{b\pi}H_{n+1}^{(m)}(\beta)\right)$$

$$a_{53} = \frac{2\mu}{i\omega}\left(\left(\pi q_m^2 + \frac{n-n^2}{2\pi b^2}\right)H_n^{(m)} - \frac{q_m}{b}H_{n+1}^{(m)}\right)$$

$$a_{63} = -\frac{n\mu w}{\omega b}H_n^{(m)}$$

$m = 2$, $\alpha = 2\pi p_2$, $\beta = 2\pi q_2$.

$\left(a_{ij}\right)_{1\le i\le 6, 4\le j\le 6}$ are deduced from the below terms by using: $m = 1$, $\alpha = 2\pi p_1$, $\beta = 2\pi q_1$ and all terms will be multiplied by (-1).

Appendix B: Radial and tangential expressions velocity

Both radial and tangential velocities can be expressed by:

$$v_k^n(\vec{r},t) = \sum_{n=0}^{+\infty}\varepsilon\int_{-\infty}^{+\infty} v_k^n(r,z)J_n(2\pi Qr_0)\cos n(\theta-\theta_0) \times E(f)e^{-I2\pi ft}df$$

with

$$v_k^n(r,z) = v_k^{n,l}(r,z) + v_k^{n,t_1}(r,z) + v_k^{n,t_2}(r,z) \;;\quad k = r,\theta$$

where

$$v_r^{n,l}(r,z) = \int_0^{\infty} \mathrm{A}_l^n(p)\begin{Bmatrix} 2\pi p\left(1+X_{ll}^n(p)\right)B_3^p + \\ i2\pi w_l X_{lt_1}^n(p)\left[B_2^{q_l} - B_3^{q_l}\right] \\ +2\pi q_l X_{lt_2}^n(p)B_2^{q_l}\end{Bmatrix} e^{-i2\pi w_l z}dp$$

$$v_r^{n,t_1}(r,z) = \int_0^{\infty} \mathrm{A}_{t_1}^n(p)\begin{Bmatrix} i2\pi w_T\left(1+X_{t_1t_1}^n(p)\right)\left[B_2^{q_t} - B_3^{q_t}\right] \\ +2\pi pX_{t_1t_2}^n(p)B_2^p \\ +2\pi q_t X_{t_1l}^n(p)B_3^{q_t}\end{Bmatrix} e^{-i2\pi w_t z}dp$$

$$v_r^{n,t_2}(r,z) = \int_0^{\infty} \mathrm{A}_{t_2}^n(p)\begin{Bmatrix} 2\pi p\left(1+X_{t_2t_2}^n(p)\right)B_2^p + \\ i2\pi w_t X_{t_2t_1}^n(p)\left[B_2^p - B_3^p\right] \\ +2\pi q_t X_{t_2l}^n(p)B_3^{q_t}\end{Bmatrix} e^{-i2\pi w_t z}dp$$

and

$$v_\theta^{n,l}(r,z) = \int_0^{\infty} \mathrm{A}_l^n(p)\begin{Bmatrix} -2\pi p\left(1+X_{ll}^n(p)\right)B_2^p + \\ i2\pi w_l X_{lt_1}^n(p)\left[B_2^{q_l} - B_3^{q_l}\right] \\ -2\pi q_l X_{lt_2}^n(p)B_3^{q_l}\end{Bmatrix} e^{-i2\pi w_l z}dp$$

$$v_\theta^{n,t_1}(r,z) = \int_0^{\infty} \mathrm{A}_{t_1}^n(p)\begin{Bmatrix} i2\pi w_t\left(1+X_{t_1t_1}^n(p)\right)\left[B_2^p - B_3^p\right] \\ -2\pi pX_{t_1t_2}^n(p)B_3^p \\ -2\pi q_t X_{t_1l}^n(p)B_2^{q_t}\end{Bmatrix} e^{-i2\pi w_t z}dp$$

$$v_\theta^{n,t_2}(r,z) = \int_0^{\infty} \mathrm{A}_{t_2}^n(p)\begin{Bmatrix} -2\pi p\left(1+X_{t_2t_2}^n(p)\right)B_3^p + \\ i2\pi w_t X_{t_2t_1}^n(p)\left[B_2^p - B_3^p\right] \\ -2\pi q_t X_{t_2l}^n(p)B_2^{q_t}\end{Bmatrix} e^{-i2\pi w_t z}dp$$

References

[1] J. M. Danthez, M. Deschamps et A. Gérard, "Réponse spatio-temporelle d'un guide cylindrique solide à un faisceau borné. I. Partie théorique", *J. Acoustique 64,* 119-125 (1989).

[2] L.Laguerre, A. Grimault and M. deschamps, "Ultrasonic transient bounded-beam propagation in solid cylinder waveguide embedded in a solid medium", *J. Acoust. Soc. Am. 121*, 1924-1934 (2007).

[3] T. R. Meeker and A. H. Meitzler, "Guided Wave Propagation in Elongated Cylinders and plates", *Physical Acoustics, Mason* (1964).

[4] J. Li and J. L. Rose, "Excitation and propagation of non-axisymmetric guided waves in a hollow cylinder", *J. Acoust. Soc. Am. 109(2),* 457-467 (2001).

[5] J.J. Ditri, "Excitation of Guided Wave Modes in Hollow cylinders by Applied surface tractions", *J. Appl. Phys. 72(7),* 2589-2597 (1992)

[6] W. C. Chew and J.A. Kong "Resonance of nonaxial symmetric modes in circular microstrip disk antenna", *J. Math. Phys. 21*, 2590-2598 (1980).

[7] E. Kausel, "Fundamental solutions in Elastodynamics: A Compendium", *Cambridge University Press*,(2006)

[8] J. A. Stratton, " Electromagnetic theory", *Mcgraw-Hill company , New York and London*, (1941)